International Journal of Nanomedicine

Dovepress

open access to scientific and medical research

Open Access Full Text Article

ORIGINAL RESEARCH

Near-Infrared Laser-Triggered, Self-Immolative Smart Polymersomes for in vivo Cancer Therapy

This article was published in the following Dove Press journal:
International Journal of Nanomedicine

Qing Tang[1,*]
Ping Hu[1,2,*]
Haibo Peng[1]
Ning Zhang[1]
Qiang Zheng[1]
Yun He[1]

[1]School of Pharmaceutical Sciences and Chongqing Key Laboratory of Natural Drug Research, Chongqing University, Chongqing 401331, People's Republic of China; [2]School of Pharmacy, Jinan University, Guangzhou 510632, People's Republic of China

*These authors contributed equally to this work

Purpose: Traditional chemotherapy is accompanied by significant side effects, which, in many aspects, limits its treatment efficacy and clinical applications. Herein, we report an oxidative responsive polymersome nanosystem mediated by near infrared (NIR) light which exhibited the combination effect of photodynamic therapy (PDT) and chemotherapy.

Methods: In our study, poly (propylene sulfide)$_{20}$-bl-poly (ethylene glycol)$_{12}$ (PPS$_{20}$-*b*-PEG$_{12}$) block copolymer was synthesized and employed to prepare the polymersome. The hydrophobic photosensitizer zinc phthalocyanine (ZnPc) was loaded in the shell and the hydrophilic doxorubicin hydrochloride (DOX·HCl) in the inner aqueous space of the polymersome.

Results: Under the irradiation of 660 nm NIR light, singlet oxygen $^1O_2$ molecules were generated from ZnPc to oxidize the neighbouring sulfur atoms on the PPS block which eventually ruptured the intact structure of polymersomes, leading to the release of encapsulated DOX·HCl. The released DOX and the $^1O_2$ could achieve a combination effect for cancer therapy if the laser activation and drug release occur at the tumoral sites. In vitro studies confirmed the generation of singlet oxygen and DOX release by NIR irradiation. In vivo studies showed that such a combined PDT-chemotherapy nanosystem could accumulate in A375 tumors efficiently, thus leading to significant inhibition on tumor growth as compared to PDT (PZ group) or chemotherapy alone (DOX group).

Conclusion: In summary, this oxidation-sensitive nanosystem showed excellent anti-tumor effects by synergistic chemophotodynamic therapy, indicating that this novel drug delivery strategy could potentially provide a new means for cancer treatments in clinic.

Keywords: near infrared laser, photodynamic therapy, oxidation-responsive, polymersome, combination therapy, cancer

Introduction

With increasing incidence and mortality, cancer is one of the leading causes of death in the world and a major public health problem.[1] In particular, melanoma is an aggressive malignancy that can be highly metastatic, and an estimated 178,560 cases of melanoma were diagnosed in the US in 2018.[2] Traditional cancer treatments, such as chemotherapy, cause severe side effects resulted from its non-specific characteristics in vivo. Effective and safe treatments for cancer are in urgent need.

Over the past few decades, organic or inorganic nanocarriers, such as micelles, polymersomes, and mesoporous silicon nanomaterials, have been developed to deliver chemotherapeutic drugs to tumor sites.[3,4] These nanocarriers can be employed alone or in combination with other new cancer treatment strategies to achieve improved therapeutic effect.[5,6] Among these new treatments, photodynamic therapy (PDT) is a promising treatment and has been approved by the FDA for

Correspondence: Yun He
School of Pharmaceutical Sciences and Chongqing Key Laboratory of Natural Drug Research, Chongqing University, 55 South Daxuecheng Road, Chongqing 401331, People's Republic of China
Tel +86 23 6567 8450
Fax +86 23 65678455
Email yun.he@cqu.edu.cn

submit your manuscript | www.dovepress.com
DovePress
http://doi.org/10.2147/IJN.S224502

clinical applications. PDT requires O_2, photosensitizers and laser irradiation with specific wavelength to produce singlet oxygen, which destroys the structure and function of target organelles through oxidative damage, causing apoptosis and necrosis of target cells.[7,8] Zinc phthalocyanine (ZnPc) is one of the widely used third-generation photosensitizer.[9,10] Höpfner et al found that tetra-triethyleneoxysulfonyl substituted zinc phthalocyanine (ZnPc) is a promising photosensitizer for photodynamic treatment of esophageal cancer, and the growth inhibition of esophageal adenocarcinoma and squamous carcinoma using ZnPc (1–10 μM) under laser irradiation was >90%.[11]

Though traditional nanocarriers can accumulate drugs at the lesion sites, they still face the challenge to effectively release the drugs from the carriers.[12] New types of nanocarriers have been introduced to address this problem, and environment-responsive carriers, such as pH responsive, temperature responsive and ROS responsive nanocarriers have been developed. Thioether-based oxidation-sensitive materials are the most studied ROS-responsive materials.[8,13] Hubble and his collaborators discovered that the hydrophobic sulfide part of poly (propylene sulfide) (PPS) underwent a phase change under oxidizing environment, forming hydrophilic sulfoxide and sulfone, resulting in a sudden hydrophobic-hydrophilic transition and rapid decomposition of the material. They also found that the PPS-*b*-PEG polymer could spontaneously form polymersomes in aqueous solution when the hydrophobic PPS and the hydrophilic PEG were in a proper ratio, which retained the hydrophobic-hydrophilic conversion ability under oxidizing conditions.[14–16]

Based on this kind of ROS-sensitive polymers as nano-drug carriers, the use of photosensitizers as a source of ROS to achieve a combination of chemotherapy and photodynamic therapy has shown great potential. In recent studies, Yu and Li,

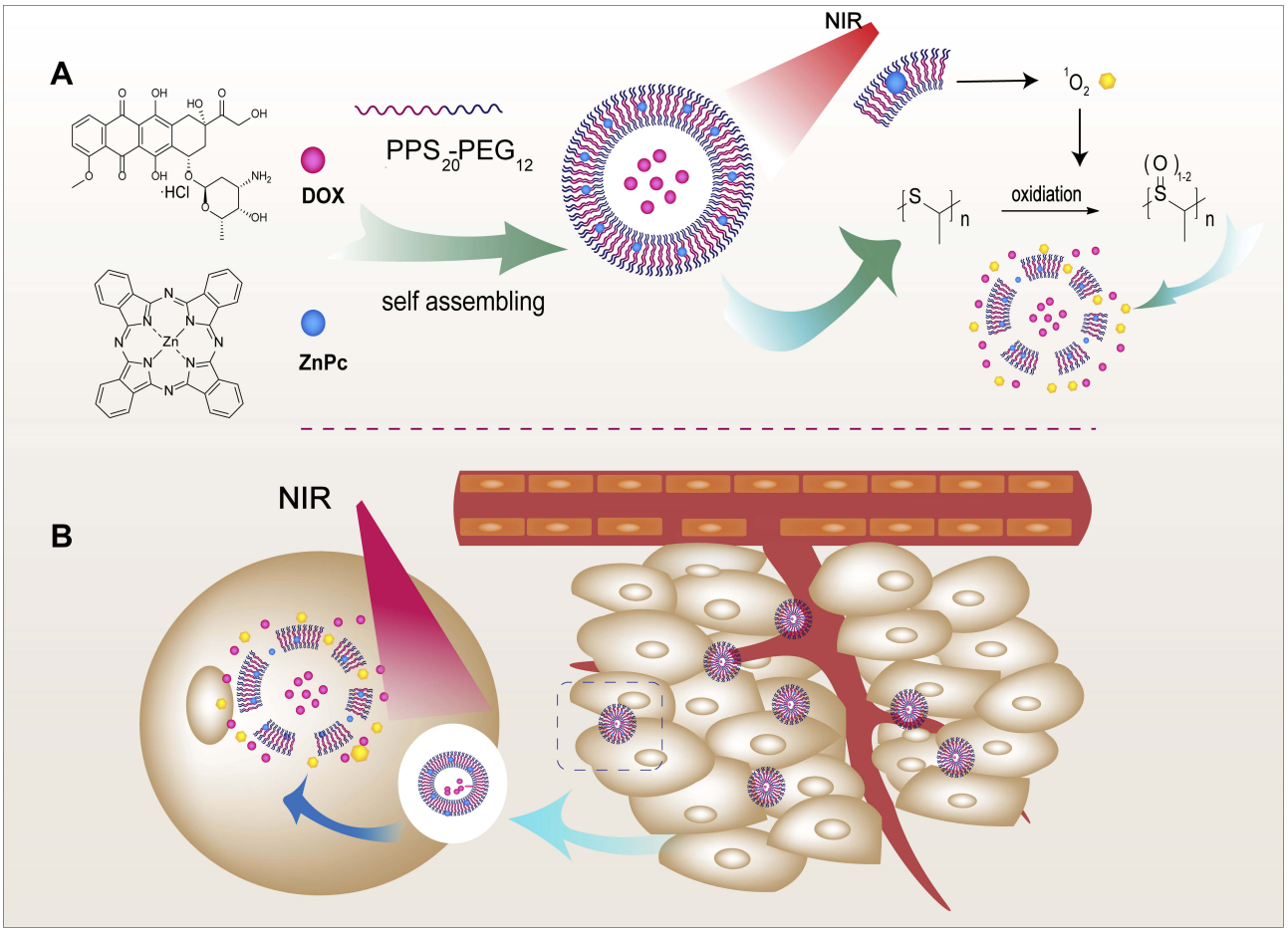

Scheme 1 Illustration of DOX and ZnPc co-loaded polymersomes and their anti-tumor behaviors in vivo. (**A**) Concepts and schematics of DOX and ZnPc co-loaded PPS-*b*-PEG polymersomes and the mechanisms of oxidation behavior upon NIR irradiation. (**B**) Schematic illustration of the intravenous polymersomes aggregated at tumor sites and dissociated to release encapsulated drugs upon NIR laser irradiation to achieve the combination effect of PDT and chemotherapy.
Abbreviations: DOX, doxorubicin hydrochloride; ZnPc, Zinc phthalocyanine; NIR, Near-infrared.

respectively, reported a nanoparticle/micelle system with selenophenyl ether or thioketal as ROS-responsive polymer/fragment and chlorin Ce6 as photosensitizer, both of them showed the abilities to kill tumors by chemophotodynamic therapy.[17,18] However, the ability to encapsulate only hydrophobic drugs and lower drug loadings limit their further applications. Therefore, continuing our efforts in searching for effective therapeutics,[19–23] we designed an oxidative responsive nanosystem mediated by NIR, which exhibited combination effect of PDT and chemotherapy. As shown in Scheme 1, a suitable proportion of PPS-PEG was used as a primary material for the nanosystem. Photosensitizer zinc phthalocyanine (ZnPc) was entrapped in the organic layer during polymersome formation, and the water-soluble doxorubicin hydrochloride (DOX HCl) was encapsulated in the polymersomes.

We investigated the synthesis of the polymer, preparation and characterizations of the ZnPc and DOX co-loaded polymersomes. The uptake and cytotoxicity of the polymersomes were systematically investigated in vitro, and their in vivo efficacy was studied using nude mice bearing malignant melanoma (A375 cells). Under the NIR laser irradiation, singlet oxygen,^{1O2} a strong oxidant generated from ZnPc, oxidized PPS and ruptured the polymersome structure, leading to the release of doxorubicin. The excess singlet oxygen generated at the tumor site caused additional damage to the tumors, achieving a combination effect of chemotherapy and photodynamic therapy.

Materials and Methods

Reagents

2-Mercaptotethanol, tris-*n*-butylphosphine (TBP), 1,8-diazabicyclo [5.4.0] undec-7-ene (DBU) and doxorubicin hydrochloride (DOX·HCl) were purchased from Energy Chemical (China). Propylene sulfide (PS) and Zinc Phthalocyanine (ZnPc) were purchased from TCI (Shanghai Development Co. Ltd). Poly (ethylene glycol) methyl ether methacrylate (average Mn 500) was purchased from Merck Life Science (Shanghai) Co. Ltd. Tetrahydrofuran (THF) and dimethyl sulfoxide (DMSO) were purchased from Chengdu Kelong Chemical Co. Ltd. DiD dye was purchased from AAT Bioquest (USA). MTT cell proliferation and cytotoxicity assay kits were purchased from Sangon Biotech (Shanghai) Co. Ltd. Hoechst 33,258 penicillin and streptomycin sulfate were obtained from Beyotime Biotechnology (China). Dulbecco's modified Eagle's medium (DMEM, high glucose) and fetal bovine serum (FBS) were obtained from Hyclone (China) and used as received. Ultrapure water was used in all experiments.

Cell Lines and Animals

Malignant Melanoma (A375) cells were obtained from the cell bank of the Chinese Academy of Sciences (Shanghai, China). The male athymic BALB/c nude mice (4–6 weeks of age, 16–20 g) were all purchased from Hunan Silaike Jingda Experimental Animal Co., Ltd. (China). Animals received care in accordance with the Guidance Suggestions for the Care and Use of Laboratory Animals.

All animal experiments were approved by the Laboratory Animal Welfare and Ethics Committee of the Chongqing University and the animal-handling procedures were followed the guidelines set by the Animal Care Committee, Chongqing University.

Synthesis and Characterization of PPS_{20}-b-PEG_{12}

Poly (propylene sulfide)$_{20}$-bl-poly (ethylene glycol)$_{12}$ was synthesized following our previous work with modifications.[20,21] Briefly, 2-mercaptoethanol (0.5 mmol, 39 mg), tris-*n*-butylphosphine (TBP, 2.5 mmol, 625 μL) and 1.8-diazabicyclo [5.4.0] undec-7-ene (DBU, 0.525 mmol, 78 μL) were added in dry THF (about 30 mL) in a Schlenk tube under an argon atmosphere. After stirring at room temperature for 5 mins, propylene sulfide (PS, 10 mmol, 1488 μL) was added dropwise and left to stir for 2 hrs. Then, poly (ethylene glycol) methyl ether methacrylate (PEG_{12}, 0.575 mmol, 274 μL) was added into the reaction solution and the reaction mixture was stirred overnight. The THF solvent was removed by roto evaporation, and the final product was precipitated in *n*-hexane.

^{1}H-NMR spectra were obtained on a Bruker Avance 400 MHz instrument. The $CDCl_3$ singlet at 7.26 ppm was selected as the reference. Molecular weight and molecular weight distribution were determined by gel permeation chromatography (GPC). An Agilent GPC was equipped with a 1260 Infinity Isocratic Pump and an RI detector. Two Agilent PL gel mixed-E columns were used with DMF containing 0.1 mol % LiBr at 30 °C at a flow rate of 1.0 mL/min. Linear poly (methyl methacrylate) from Fluka was used as the standard for calibration. Aliquots of the polymer samples were dissolved in DMF/LiBr (1 mg/mL).

PPS_{20}-*b*-PEG_{12} ^{1}H-NMR ($CDCl_3$, 400MHz): 1.31–1.40 (-C*H*$_3$ in PPS chain), 2.50–2.69 (1 diastereotopic H of -C*H*$_2$- in

PPS chain), 2.77–2.98 (2H, -S-CH_2-CH_2-COO-, -CH- and 1 diastereotopic H of -CH_2- in PPS chain), 3.22–3.34 (-CH_3 in PEG chain), 3.55–3.74 (-CH_2- in PEG chain), 4.18–4.3 (-CH_2-CH_2-).

Preparation of ZnPc and DOX-Loaded PPS_{20}-b-PEG_{12} Polymersomes

ZnPc and DOX·HCl loaded PPS_{20}-*b*-PEG_{12} polymersomes (PZD) were formed by solvent dispersion method. For this method, Zinc Phthalocyanine (ZnPc) was first separately dissolved in DMSO at 500 μg/mL, DOX·HCl was dissolved in ultrapure water at 100 μg/mL, and the polymer/ZnPc molar ratio during polymersome formation was 20:1. During solvent dispersion, PPS_{20}-*b*-PEG_{12} (20 mg) was dissolved in THF with the addition of ZnPc solution and added dropwise to ultrapure water at a speed of 0.25 mL/min, and the ratio of DMSO/THF/water was 0.01:0.1:1 followed by desiccation to remove the THF. Unloaded DOX, residual DMSO and THF were removed by dialysis. We also prepared polymersomes loaded only with ZnPc (PZ) following the same method by just replacing the DOX·HCl water solution with ultrapure water.

The size of polymersomes was characterized with dynamic light scattering (DLS; Malvern, Zetasizer Nano Series 90) at a concentration of approximately 1 mg/mL. The morphology of the micelle was characterized by Cryogenic transmission electron microscopy (Cryo-TEM, FEI, TF20, USA).

A UV–visible spectrophotometer was used to determine the total loading contents of DOX and ZnPc. 0.1mL Drug-loaded polymersomes were dissolved in 2 mL of DMSO, and the readings were recorded at 480 nm and 675 nm wavelengths, respectively. The concentrations of DOX and ZnPc were calculated according to the calibration curve of different drugs. The drug loading (DL) and encapsulation efficiency (EE) were calculated by the following equations:

$$\mathrm{DL}(wt\%) = \frac{w\ (\text{drug in polymersomes})}{w\ (\text{total polymersomes})} \times 100\%$$

$$\mathrm{EE}(wt\%) = \frac{w\ (\text{drug in polymersomes})}{w\ (\text{initial drug added})} \times 100\%$$

Oxidization Behavior of Polymersomes Upon Laser Irradiation

Two milliliters of drug-loaded polymersome suspension (ZnPc concentration: 15 μg/mL) were irradiated with a 660 nm (±5 nm) laser irradiation for 10 mins, the laser power was 100 mW/cm^2 and the suspension was then lyophilized and subjected to ^{1}H-NMR analysis to determine if the PPS peaks were changed.

In vitro Controlled Drug Release Profiles of Polymersomes

The in vitro release profiles of DOX from drug-loaded polymersomes containing DOX in the presence or absence of 660 nm laser irradiation were explored. Briefly, PZD solutions (2 mL) including 0.3 mg DOX were sealed in a dialysis bag with a MWCO of 2000 and incubated in 18 mL ultrapure water with or without He-Ne laser irradiation (100 mW/cm^2) for 20 mins at 0 h, 2 h,4 h, 8 h,12 h and 24 h. Periodically, 2 mL of release media were taken out for measurement and replenished with an equal volume of fresh media. The release media was objected to UV–visible spectrophotometer at 480 nm to detect the DOX concentration, and the amount of DOX was determined by the DOX calibration curve obtained from the absorbance.

Detection of Singlet Oxygen Generation

3-Diphenylisobenzofuran (DPBF) is a common chemical probe to detect singlet oxygen generation. DPBF can combine with singlet oxygen to gradually lose its characteristic absorption peak at 415 nm. In a typical experiment, 20 μL of DPBF (1000 ppm in DMF) was added to 2 mL of PZD suspension in a quartz cuvette. The cuvette was kept in dark and irradiated with a 660 nm He-Ne laser at a power of 100 mW/cm^2, and the absorption spectrum was recorded at 0 s, 30 s, 60 s, 150 s and 300 s. The rate of singlet oxygen generation was determined by the reduction of DPBF absorbance over time. Irradiation of ZnPc in the absence of free polymersomes was also carried out and set as a positive control.

Cellular Uptake

Confocal laser scanning microscopy (CLSM) was used to evaluate the cellular internalization and intracellular distribution of free ZnPc, free DOX, PZ, DOX-loaded polymersomes (PD) and PZD. Typically, A375 cells were plated onto 24-well glass bottom Petri dishes at a density of 1×10^5 cells per dish, and then incubated for 24 h at 37 °C in CO_2/air (5/95). DMEM was then removed and washed with PBS twice, 500 μL fresh medium containing free DOX (3 μg/mL), and free ZnPc (3 μg/mL), PZ (3 μg/mL), PD (3 μg/mL) or PZD (DOX: 3 μg/mL, ZnPc: 3 μg/mL) were added afterwards. After incubation for additional 2 hrs, the

original DMEM was removed and the cells were washed carefully with cold PBS thrice, and immobilized in 4% paraformaldehyde for 20 mins. The nuclei were next counter-stained with Hoechst 33,258 and observed by CLSM. The DOX was excited at 488 nm and monitored at 570–620 nm, the ZnPc was excited at 633 nm and monitored at 640–735 nm, and the Hoechst 33,258 was excited at 405 nm and monitored at 430–500 nm.

Flow cytometry was used to further determine the total fluorescence intensity of A375 cells incubated with different

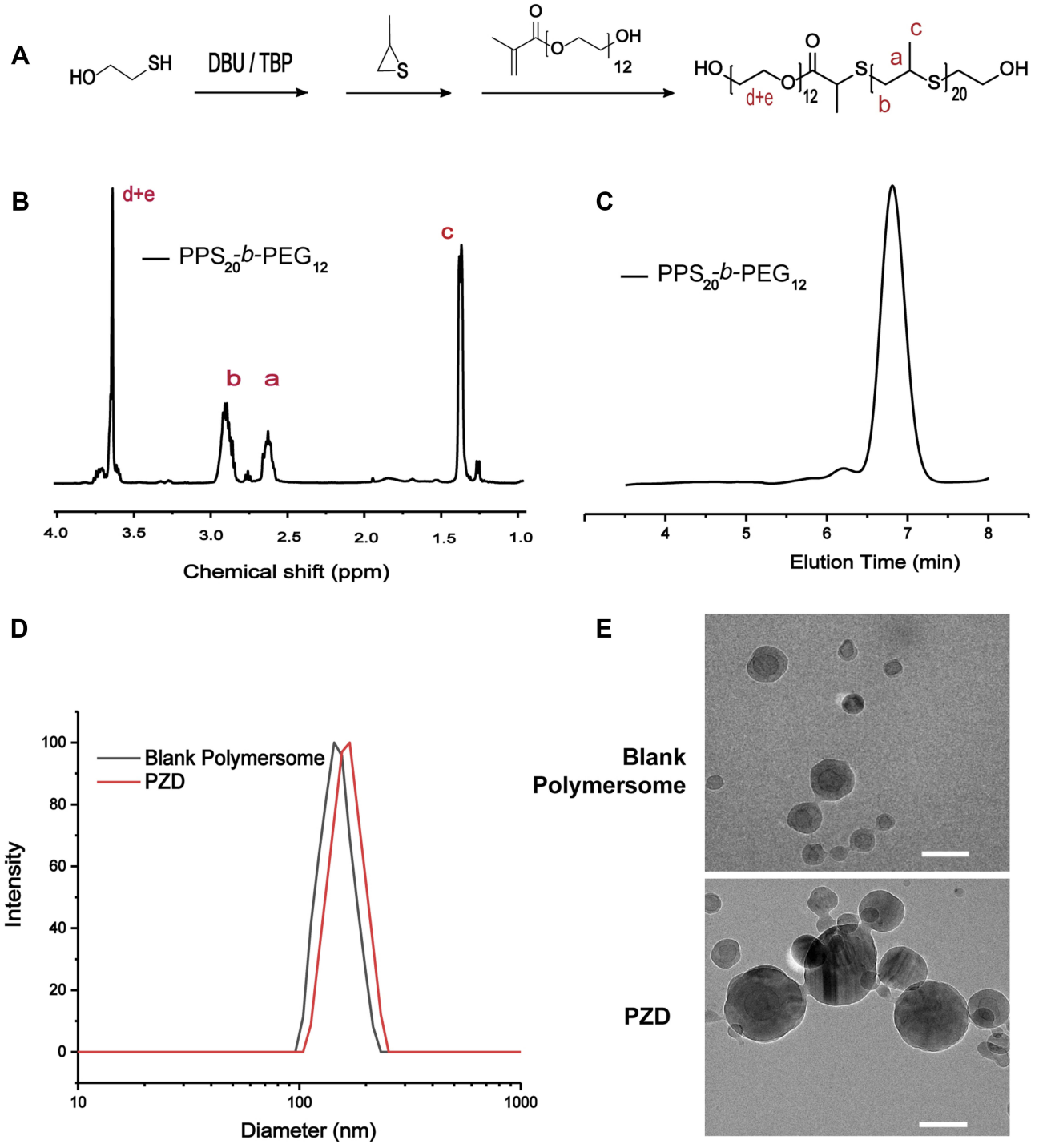

Figure 1 Characterization of PPS_{20}-*b*-PEG_{12}. (**A**) Synthesis of PPS-*b*-PEG copolymers. (**B**) ^{1}H-NMR spectrum of PPS_{20}-*b*-PEG_{12} copolymers. (**C**) GPC traces of PPS_{20}-*b*-PEG_{12} copolymers. (**D**) Size distribution of free polymersomes, ZnPc and DOX coloaded polymersomes (PZD) by Brookhaven NanoBrook 90Plus Particle Size Analyzer. (**E**) Cryo-TEM images of PZD, scale bar represents 100 nm.

Abbreviations: DOX, doxorubicin hydrochloride; ZnPc, Zinc phthalocyanine; PZD, ZnPc and DOX coloaded polymersomes.

samples. Briefly, A375 cells (2×10^6 cells/well) were seeded in a 6-well plate and cultivated for 24 h for full adhesion. The media was replaced with a fresh media containing free DOX (3 μg/mL), free ZnPc (3 μg/mL), PZ (3 μg/mL), PD (3 μg/mL) or PZD (DOX: 3 μg/mL, ZnPc: 3 μg/mL) respectively. The free DMEM was used as the control. After 2 hrs, the cells were washed with PBS three times and harvested with trypsin digestion. The cells were then examined by flow cytometry. The DOX was measured into the PE-A channel, while the ZnPc was measured into the APA-A700-A channel.

In vitro Cytotoxicity Studies of Drug-Loaded Polymersomes

The chemotherapy-PDT performance was evaluated by MTT assays. Briefly, A375 cells (1×10^4 cells per well) were seeded into three 96-well plates and incubated for 24 h, cells were treated with different concentrations of free DOX, free ZnPc, PZ, PD, and PZD, respectively. The concentrations of free DOX, free ZnPc, PZ and PD were 2, 4, 6, 8 and 10 μg/mL, while PZD contained 1, 2, 3, 4, 5 μg/mL DOX and ZnPc, respectively. To evaluate the photo- and dark-toxicity of drug-loaded polymersomes, these plates were irradiated with or without 660 nm He-Ne laser (100 mW/cm^2) for 10 mins after a 4-hr incubation. The MTT reagent (5 mg/mL) was used to determine the cell viability after additional incubation for 20 hrs.

In vivo Fluorescence Imaging and Biodistribution

Since photosensitizer ZnPc was not a suitable dye for fluorescence imaging in vivo, we prepared polymersomes containing fluorescent dye DiD, named P-DiD. The mice were injected with 1 mg/kg DiD via tail vein. Images and quantitative fluorescence analysis of DiD were taken at 0 h, 0.5 h, 2 h, 4 h, and 6 h after injection using the in vivo imaging system (PerkinElmer, IVIS Spectrum, USA) to collect the fluorescence signals of DiD with a 640 nm excitation wavelength and a 680 nm filter.

All mice were sacrificed at 6 h post-dose administration, and the excised healthy organs (livers, lungs, spleens, hearts and kidneys) together with tumors were collected for imaging and fluorescence recording.

In vivo Antitumor Efficacy

The male athymic BALB/c nude mice (4–6 weeks of age, 16–20 g) were used for xenografted tumor implantation. 200 μL A375 cells ($1*10^7$) were administered by subcutaneous injection into the armpit region of the mice to grow. The tumor volume was calculated as follows:

$$\text{tumor volume} = \frac{(\text{tumor length}) \times (\text{tumor width})^2}{2}$$

After the tumors were successfully implanted, the mice were randomized into five groups (five mice per group) for the following treatments: (group I) 150 μL of saline injected intravenously; (group II) 150 μL of PZ (1 mg/kg) injected intravenously; (group III) 150 μL of PZD (1 mg/kg) injected intravenously; (group IV) 150 μL of free DOX (1 mg/kg) injected intravenously; (group V) 150 μL of saline injected intravenously and irradiated with 660 nm He-Ne laser for 30 mins. The tumor area of group II, group III and group V were irradiated with 660 nm He-Ne laser for 30 mins at 100 mW/cm^2 after 4 hrs of injection. The drug injections were repeated after 3 days. Changes in mouse body weight and tumor volume were recorded every 2 days.

Results

Structural and Morphological Characterizations of Polymersomes in vivo Antitumor Efficacy

The amphiphilic PPS-*b*-PEG block copolymers were synthesized by living anionic polymerization of propylene sulfide using a small molecular initiator. The synthetic route was shown in Figure 1A, and the structure of PPS-*b*-PEG copolymers was verified by ^{1}H-NMR in $CDCl_3$ (Figure 1B), and the molecular weight distribution of the PPS-*b*-PEG copolymers was determined by GPC (Figure 1C). Both the calculated molecular weight and the narrow PDI of the copolymers (1.16, Table S1) further demonstrated the successful synthesis of the copolymer.

PPS_{20}-*b*-PEG_{12} copolymers, possessing a comparable ratio of the hydrophobic and hydrophilic blocks, were designed to self-assemble into polymersomes in aqueous solution. The hydrodynamic diameter of the formed structure was detected by dynamic light scattering (DLS). The results showed that the size of the blank polymersomes was about 130 nm and increased to ~150 nm when the polymersomes were co-encapsulated with ZnPc and DOX (Figure 1D). Cryo-transmission electron microscopy (Cryo-TEM) further revealed the shape and size of the polymersomes and confirmed the detailed structure of the hollow spheres (Figure 1E).

Co-loading of ZnPc and DOX into the polymersomes were crucial for PDT and chemotherapy in this study and

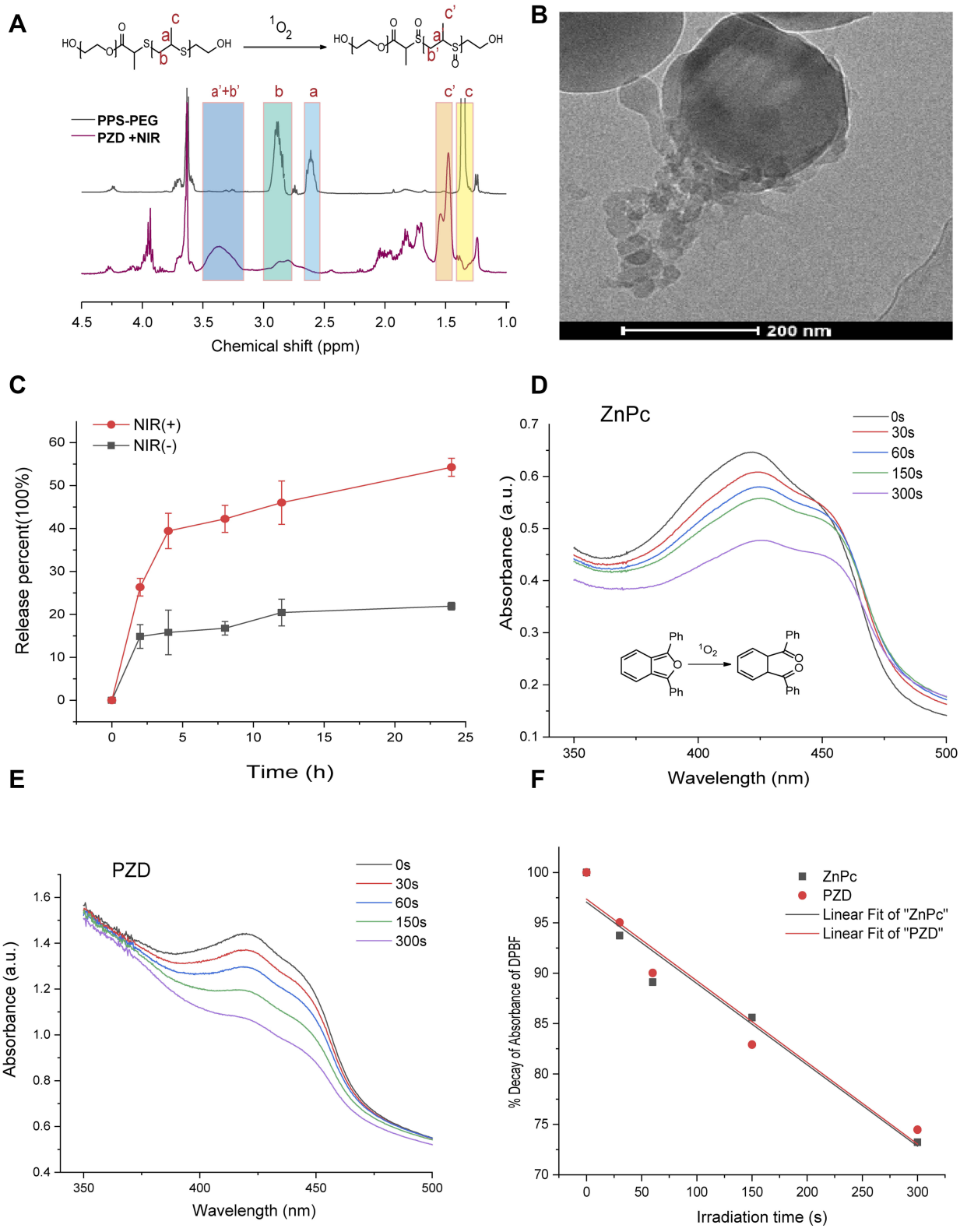

Figure 2 Characterization of the oxidative behaviors of PZD polymersomes. (**A**) ^{1}H-NMR spectra of the copolymers from PZD before and after laser irradiation. (**B**) Cryo-TEM figure of NIR-irradiated polymersomes, scale bar represents 100 nm. (**C**) DOX release from PZD in the presence or absence of laser irradiation. (**C**) Schematic diagram of DBPF reaction with singlet oxygen. (**D**) Singlet oxygen produced from ZnPc (5 μg/mL) over time. (**E**) Singlet oxygen produced from PZD (ZnPc: 5 μg/mL) over time. (**F**) The decay of the absorbance of DPBF.

Abbreviations: DOX, doxorubicin hydrochloride; ZnPc, Zinc phthalocyanine; PZD, ZnPc and DOX coloaded polymersomes; Cryo-TEM, Cryo-transmission electron microscopy; DBPF, 3-Diphenylisobenzofuran.

the drug loading was measured by UV-vis for their distinctive absorbance. The samples of the drug loaded polymersome dispersions were dissolved in the DMSO solution and their absorbance was then measured. The drug loading (DL) of DOX and ZnPc were 5.44% and 2.45% respectively, and the encapsulation efficiency (EE) of DOX and ZnPc were 41.01% and 69.62%, respectively (Table S2).

The generation of singlet oxygen from ZnPc under NIR irradiation was reported.[24,25] We demonstrated that the singlet oxygen generated from ZnPc was sufficient to oxidize the hydrophobic PPS chain and initiate the drug release in our polymersome system. Thus, 2 mL of PZD suspension (ZnPc concentration: 15 μg/mL) was irradiated with a 660 nm (±5 nm) laser at a power of 100 mW/cm^2 for 10 mins, and the suspension was then lyophilized and subjected to ^{1}H-NMR measurements to observe the chemical shifts of the PPS. Our NMR studies in Figure 2A showed the decrease of the original PPS block signals (peaks a, b and c highlighted in grey) and the newly appearance of peaks a', b' and c' (highlighted in red), which are close to the chemical shifts of hydrogens in sulfone and sulfoxide. Figure 2B illustrates the decomposition of polymersomes after irradiation with NIR laser, which complemented the results obtained in Figure 2A. All these results confirmed that the singlet oxygen produced from ZnPc oxidized the PPS block and induced the breakdown of the polymersomes.

The in vitro release of DOX from PZD in the presence or absence of 660 nm laser irradiation was investigated using a dialysis bag method. The DOX concentration of the release media was measured at 480 nm on a UV–visible spectrophotometer. As shown in Figure 2C, NIR-irradiated PZD had more than 50% DOX release after 24 hrs, while the non-irradiated PZD showed less than 20%.

3-Diphenylisobenzofuran (DPBF), a commonly used probe to capture singlet oxygen, was employed to examine the rate and quantity of singlet oxygen produced from ZnPc.[26] Singlet oxygen can react with DPBF and lead to a gradual disappearance of the characteristic absorption peak of DPBF at 415 nm. According to Figure 2D–F, the decrease of the absorption peak confirmed the generation of singlet oxygen, and the PZD samples showed reduced rate and quantity of singlet oxygen production, possibly due to the partial consumption of the produced singlet oxygen by PPS.

In vitro Cell Uptake and Cytotoxicity Studies

The cellular uptake of free DOX, free ZnPc, PZ (ZnPc loaded polymersomes) PD (DOX-loaded polymersomes), PZD (ZnPc and DOX co-loaded polymersomes) by A375 cells at 3 μg/mL was examined using confocal microscopy (Figure 3A). As shown in Figure 3A, ZnPc and DOX were accumulated in the cytoplasm and nucleus, respectively, regardless of whether they were encapsulated by polymersomes, while free ZnPc and free DOX showed the strongest fluorescence intensity. However, the fluorescence intensity of the PZ and PZD groups were difficult to distinguish. Flow cytometry was employed to quantify the fluorescence intensity of each sample. As shown in Figure 3B–C, free DOX and free ZnPc also exhibited the strongest fluorescence intensity. However, the PZD group showed different results in different channels. Since the DOX/ZnPc concentrations contained in the different components are identical, for the PZD group, the fluorescence intensity of DOX or ZnPc should be theoretically similar with the PD or PZ group. Figure 3B shows that the fluorescence intensity of DOX was almost the same in the PD and PZD groups, which was in agreement with the theoretical results. However, for the fluorescence intensity test of ZnPc, the results of flow cytometry in Figure 3C showed that the PZD group had much higher fluorescence intensity than the PZ group. After some extra fluorescence quantification by flow cytometry, we found that this kind of performance was due to the partial superposition of the fluorescence intensity of DOX and ZnPc under the used excitation/emission wavelength (Figure S1.).

The efficacy of the polymersome samples was evaluated by MTT assays. As shown in Figure 3D, the PZD and free ZnPc groups without irradiation showed insignificant toxicity to the cells even at a concentration up to 10 μg/mL (Figure 3D). The irradiated PZ group showed greater toxicity than DOX at low levels. At higher concentrations, its cytotoxicity was higher than the DOX group. The NIR light irradiated PZD showed more cytotoxicity at low concentrations while the cytotoxicity of NIR-irradiated free ZnPc was more significant at high levels. It was probable that free ZnPc produced more ROS under NIR irradiation. The cell viability of PZD containing 2 μg/mL encapsulated DOX and ZnPc was about 25%. When the concentration of DOX and ZnPc reached 5 μg/mL, the cell viability was further reduced to 10%, which was significantly lower than that of free DOX group but higher than the free ZnPc group. These results demonstrated that PZD combined photodynamic therapy and chemotherapy, and significantly improved the therapeutic efficacy compared with either chemotherapy or PDT with the irradiation of the NIR laser. The cytotoxicity of PZ (without NIR irradiation) and PD group were shown in Figure S2.

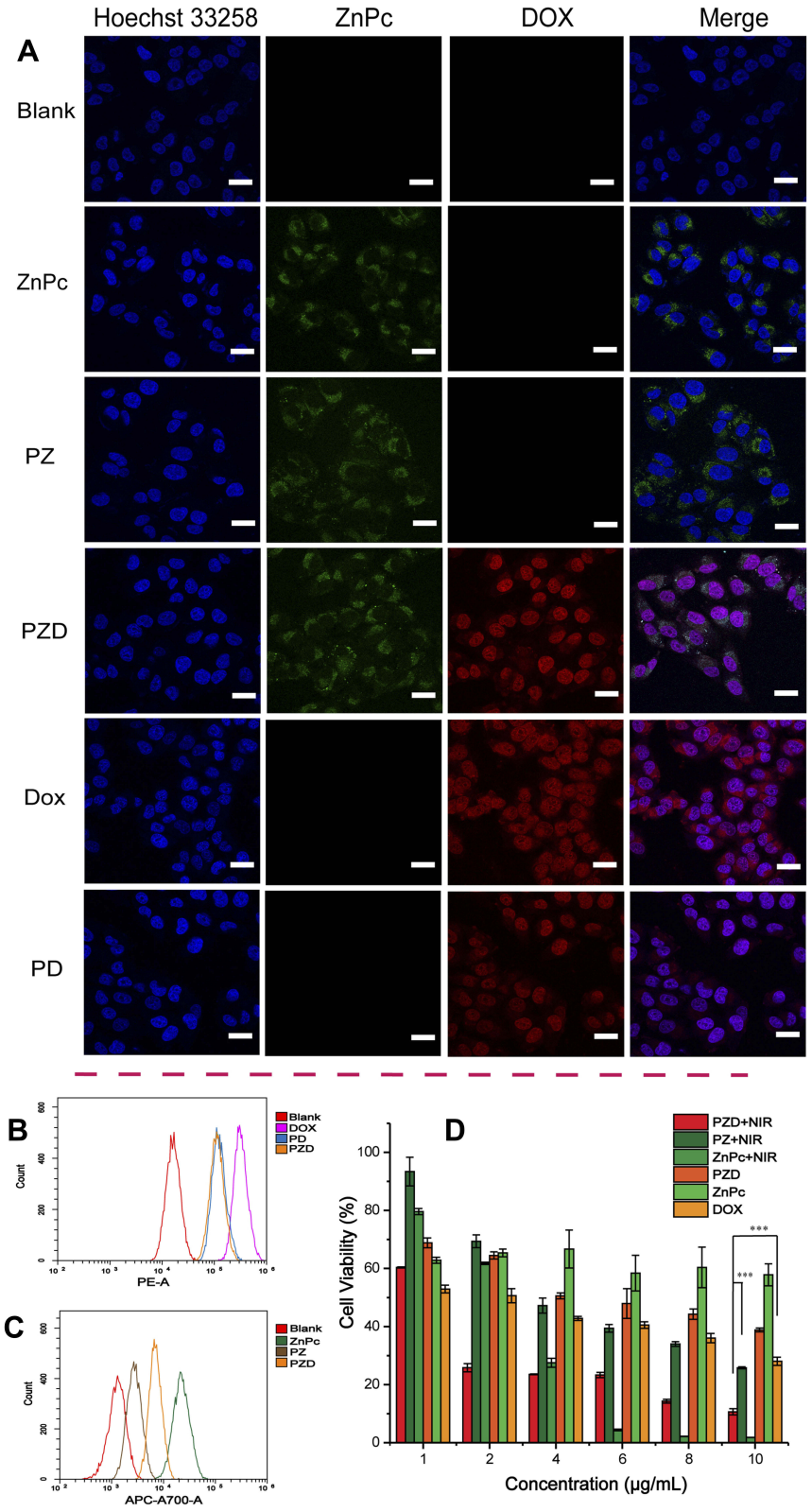

Figure 3 In vitro encapsulation and cytotoxicity performances of free DOX, free ZnPc, PZ, PD, and PZD. (**A**) Fluorescence images of A375cells incubated with free DOX, free ZnPc, PZ, PD and PZD for 2 h. Scale bar represents 25 μm. (**B**) Fluorescence intensity of DOX, PD and PZD in the PE-A channel. (**C**) Fluorescence intensity of ZnPc, PZ and PZD in the APC-A700-A channel. (**D**) Cytotoxicity of free DOX, free ZnPc, PZ, PD, and PZD with/without irradiation against A375 cells by MTT assay. (Data represent mean ± SD, n=3, Student's *t*-test, ***P<0.005).

Abbreviations: DOX, doxorubicin hydrochloride; ZnPc, Zinc phthalocyanine; NIR, Near-infrared; PZD, ZnPc and DOX coloaded polymersomes; PZ, ZnPc loaded polymersomes; PD, DOX loaded polymersomes.

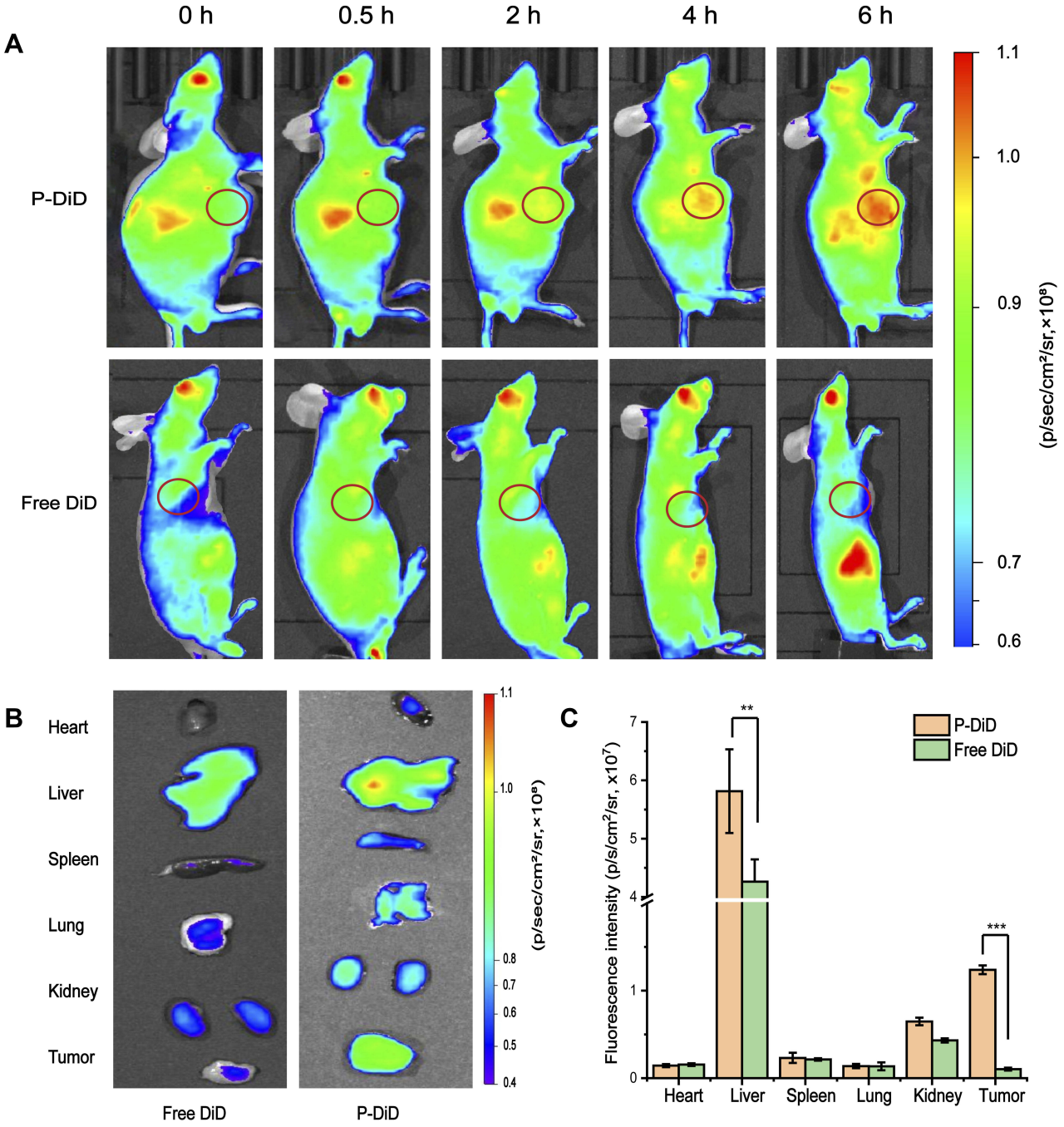

Figure 4 In vivo fluorescence imaging and biodistribution of P-DiD. (**A**) Time-dependent in vivo fluorescence images of BALB/c nude mice with A375 xenografts. Images were taken at 0, 0.5, 2, 4 and 6 h after the injection with 150 μL P-DiD via the tail vein. (**B**) Biodistribution of free DiD and P-DiD in BALB/c nude mice bearing A375 xenografts at 6 h post-injection in organs and tumor. (**C**) Quantitative analysis of DiD fluorescence intensity acquired from liver and tumor. (Data represent mean ± SD, n=3, Student's *t*-test, **P<0.01, ***P<0.005).
Abbreviation: P-DiD, DiD loaded polymersomes.

In vivo Fluorescence Imaging and Antitumor Efficacy of PZD

Biodistribution experiments were performed on tumor-bearing mice to study the distribution of nanopolymersomes in vivo. Due to the weak fluorescence intensity of ZnPc in aqueous solution, we prepared polymersomes containing a fluorescent dye DiD in the place of ZnPC, named P-DiD to monitor the biodistribution of the polymersomes.

Figure 4A illustrates that initially P-DiD was predominantly concentrated in the liver and reached its maximum in the liver at hour 2. At the same time, P-DiD began to accumulate in the tumor site and the fluorescence of the tumor site was the strongest at hour 6, indicating a considerable amount

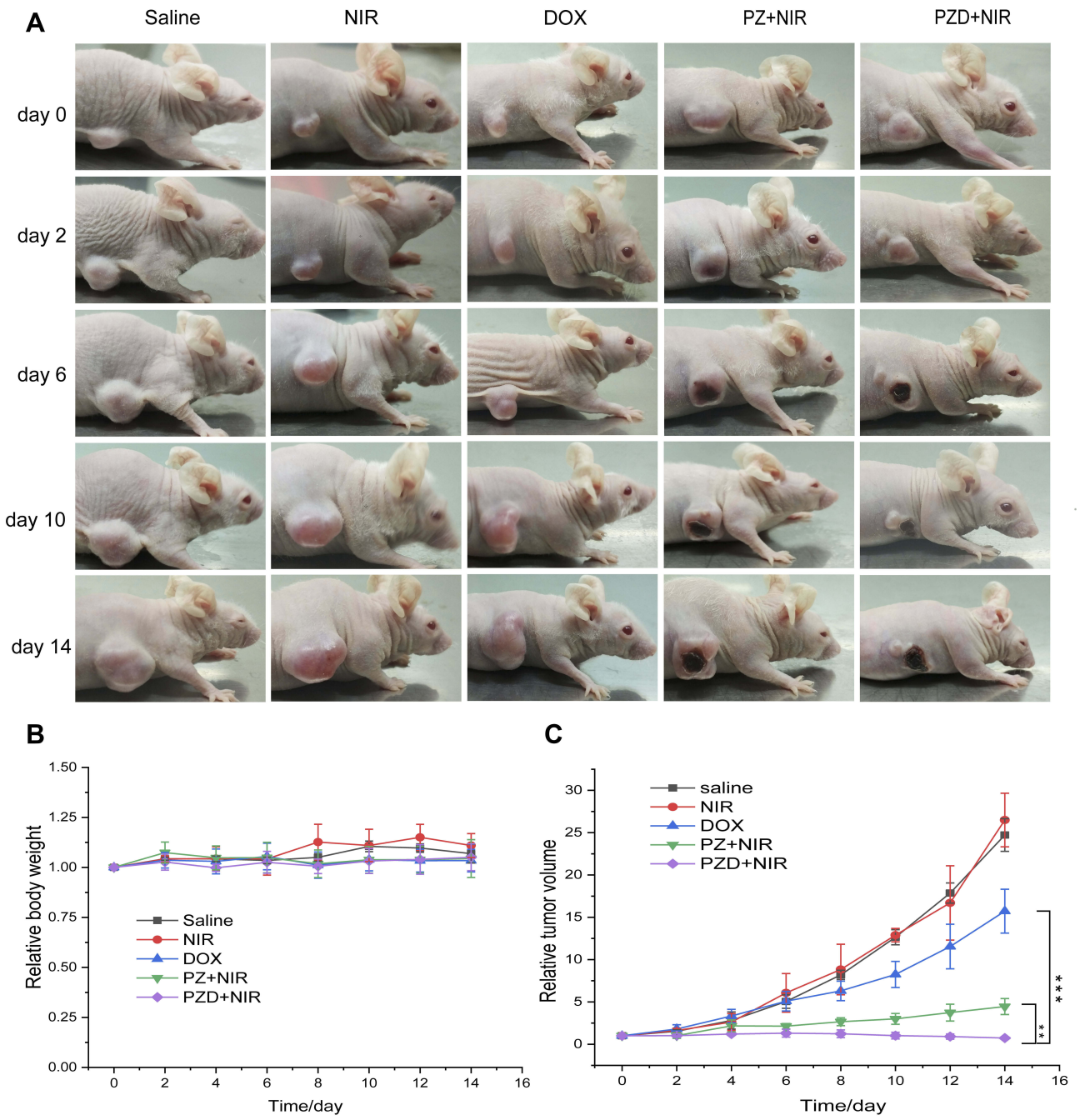

Figure 5 In vivo antitumor studies of saline, NIR, DOX, PZ and PZD groups. (**A**) Photographs of malignant melanoma (A375 cells) bearing mice during the antitumor studies (doses: 1mg/kg, 0, 2, 6, 10 and 14 days). (**B**) Body weight changes of the tumor-bearing mice measured during the antitumor studies. (**C**) Relative tumor volume changes of mice treated with saline, NIR, DOX, PZ and PZD with NIR laser irradiation. (Data represent mean ± SD, n=5, Student's *t*-test, **P<0.01, ***P<0.005).
Abbreviations: DOX, doxorubicin hydrochloride; NIR, Near-infrared; PZD, ZnPc and DOX coloaded polymersomes; PZ, ZnPc loaded polymersomes.

of P-DiD was accumulated at the tumor site after 6 hrs. The fluorescence images of organs and tumors were taken after 6 hrs and shown in Figure 4B–C. Although the liver showed the strongest fluorescence intensity, the tumor tissues from P-DiD injected mice showed increased fluorescence intensity compared to the mice injected with free DiD, possibly due to the Enhanced Permeability and Retention effect (EPR effect) of tumor tissue to capture nanosized polymersomes. Meanwhile, other organs (heart, spleen, lung and kidney) showed relatively weak fluorescence due to less accumulation of P-DiD.

The anti-tumor effect of PZD on tumor-bearing mice was then examined. Balb/c nude mice bearing malignant melanoma (A375 cells) were randomized into five groups (five mice per group) for different treatments. Compared to the

saline group, both DOX and PZ groups with NIR laser irradiation exhibited inhibition on tumor growth. The PZD group with NIR laser irradiation showed significant inhibition of tumor growth by approximately 70% after 14 days, while the laser light alone did not inhibit tumor growth (Figure 5A–C). At the same time, we also proved that this irradiation condition does not cause an increase in temperature, indicating that the tumor-killing ability is caused by PDT rather than PDT and temperature (Figure S3). The weight of the mice in different groups remained about 25 g. Since the mice in different groups had different tumor volumes, the mice from the PZD+NIR group had the least bodyweight loss, suggesting the health condition among all the study groups (Figure 5B).

Discussion

Although melanoma is a rare kind of tumor, it is one of the highly aggressive and lethal cancers with a mortality rate of 80% of the total number of skin cancers due to its high metastasis and acquired chemoresistance.[2,27] The primary treatments of melanoma are surgery, chemotherapy and radiotherapy, of which may face the dilemma of limited treatment ranges and serious side effects.[2] However, skin melanoma also shows the ability of light illuminate, making PDT a promising treatment.[28] Due to the control of illumination position and the on-demand activation of photosensitizer, PDT has better selective antitumor activities and lower side effects than conventional radiotherapy and chemotherapy. At the same time, PDT can further prevent tumor recurrence by stimulating the body's immune system to produce tumor immune memory.[27] Furthermore, the combination of traditional treatments and PDT can further reduce drug use and avoid potential side effects while ensuring efficacy. Unlike photothermal agents that have both elevated temperatures and the ability to generate singlet oxygen,[29–31]– photosensitizers are generally considered to have only the ability to produce singlet oxygen unless they possess particular morphological features.[32–34]– Therefore, we confirmed that the combination of chemotherapy and PDT is effective and feasible in our study.

By encapsulation ZnPc in the bilayers of polymersome, the water insolubility and aggregation can be avoided. The choose of oxidation-responsive drug carrier not only ensure the on-demand release of inner drugs but also provide proper biocompatibility. The killing ability of PZD for melanoma can be attributed to the effective tumor site aggregation of the EPR effect, as well as tumor cell apoptosis/necrosis caused by DOX and singlet oxygen.[17,35,36] Compared with DOX/PZ groups, the tumor growth rate was delayed, while the PZD group showed effective inhibition of tumor. Besides, the single concentration of the components in the PZD group is only half of the DOX and PZ groups. The synergetic effects of chemotherapy and photodynamic therapy can effectively enhance the tumor killing abilities.

Conclusion

We have designed and developed an ROS-sensitive nano-sized polymersome as a multifunctional platform for combinatory cancer therapy. This platform demonstrated excellent anti-tumor effects in vivo and in vitro by encapsulating a traditional photosensitizer and chemo-therapeutic agent. This nanoplatform could be conveniently used to encapsulate both hydrophilic and hydrophobic drugs. The drugs could be specifically triggered for release under the NIR irradiation. These polymersomes provided an excellent example and opportunity for on-demand cancer treatment and enhanced anticancer therapy, and could find potential applications in clinic.

Disclosure

The authors report no conflicts of interest in this work.

References

1. Bray F, Ferlay J, Soerjomataram I, Siegel RL, Torre LA, Jemal A. Global cancer statistics 2018: GLOBOCAN estimates of incidence and mortality worldwide for 36 cancers in 185 countries. *CA Cancer J Clin*. 2018;68:394–424. doi:10.3322/caac.v68.6
2. Domingues B, Lopes JM, Soares P, Pópulo H. Melanoma treatment in review. *Immunotargets Ther*. 2018;7:35–49. doi:10.2147/ITT.S134842
3. Din FU, Aman W, Ullah I, et al. Effective use of nanocarriers as drug delivery systems for the treatment of selected tumors. *Int J Nanomedicine*. 2017;12:7291–7309. doi:10.2147/IJN.S146315
4. Ma P, Xiao H, Li C, et al. Inorganic nanocarriers for platinum drug delivery. *Mater Today*. 2015;18:554–564. doi:10.1016/j.mattod.2015.05.017
5. Kuzyniak W, Schmidt J, Glac W, et al. Novel zinc phthalocyanine as a promising photosensitizer for photodynamic treatment of esophageal cancer. *Int J Oncol*. 2017;50:953–963. doi:10.3892/ijo.2017.3854
6. Kuzyniak W, Ermilov EA, Atilla D, et al. Tetra-triethyleneoxysulfonyl substituted zinc phthalocyanine for photodynamic cancer therapy. *Photodiagnosis Photodyn Ther*. 2016;13:148–157. doi:10.1016/j.pdpdt.2015.07.001
7. Li Q, Li W, Di H, et al. A photosensitive liposome with NIR light triggered doxorubicin release as a combined photodynamic-chemo therapy system. *J Control Release*. 2018;277:114–125. doi:10.1016/j.jconrel.2018.02.001
8. Sobotta FH, Hausig F, Harz DO, Hoeppener S, Schubert US, Brendel JC. Oxidation-responsive micelles by a one-pot polymerization-induced self-assembly approach. *Polym Chem*. 2018;9:1593–1602. doi:10.1039/C7PY01859B
9. Xiong W, Peng L, Chen H, Li Q. Surface modification of MPEG-b-PCL-based nanoparticles via oxidative self-polymerization of dopamine for malignant melanoma therapy. *Int J Nanomedicine*. 2015;10:2985–2996. doi:10.2147/IJN.S79605

10. Allison RR, Sibata CH. Oncologic photodynamic therapy photosensitizers: a clinical review. *Photodiagnosis Photodyn Ther*. 2010;7:61–75. doi:10.1016/j.pdpdt.2010.02.001
11. Liang R, You S, Ma L, et al. A supramolecular nanovehicle toward systematic, targeted cancer and tumor therapy. *Chem Sci*. 2015;6:5511–5518. doi:10.1039/C5SC00994D
12. Dolmans DEJGJ, Fukumura D, Jain RK. Photodynamic therapy for cancer. *Nature Rev Cancer*. 2003;3:380. doi:10.1038/nrc1071
13. Sibata CH, Colussi VC, Oleinick NL, Kinsella TJ. Photodynamic therapy: a new concept in medical treatment. *Braz J Med Biol Res*. 2000;33:869–880. doi:10.1590/S0100-879X2000000800002
14. Napoli A, Valentini M, Tirelli N, Müller M, Hubbell JA. Oxidation-responsive polymeric vesicles. *Nat Mater*. 2004;3:183. doi:10.1038/nmat1081
15. Maranho DS, de Lima RG, Primo FL, da Silva RS, Tedesco AC. Photoinduced Nitric Oxide and singlet oxygen release from ZnPC liposome vehicle associated with the nitrosyl ruthenium complex: synergistic effects in photodynamic therapy application. *Photochem Photobiol*. 2009;85:705–713. doi:10.1111/php.2009.85.issue-3
16. Zhou X, He X, Wei S, Jia K, Liu X. Au nanorods modulated NIR fluorescence and singlet oxygen generation of water soluble dendritic zinc phthalocyanine. *J Colloid Interface Sci*. 2016;482:252–259. doi:10.1016/j.jcis.2016.07.072
17. Li Y, Hu J, Liu X, et al. Photodynamic therapy-triggered on-demand drug release from ROS-responsive core-cross-linked micelles toward synergistic anti-cancer treatment. *Nano Res*. 2019;12:999–1008. doi:10.1007/s12274-019-2330-y
18. Yu L, Yang Y, Du F-S, Li Z-C. ROS-responsive chalcogen-containing polycarbonates for photodynamic therapy. *Biomacromolecules*. 2018;19:2182–2193. doi:10.1021/acs.biomac.8b00271
19. Lin Z, Xu X, Zhao S, et al. Total synthesis and antimicrobial evaluation of natural albomycins against clinical pathogens. *Nat Commun*. 2018;9:3445. doi:10.1038/s41467-018-05821-1
20. Tang M, Zheng Q, Tirelli N, et al. Dual thermo/oxidation-responsive block copolymers with self-assembly behaviour and synergistic release. *React Funct Polym*. 2017;110:55–61. doi:10.1016/j.reactfunctpolym.2016.12.009
21. Tang M, Hu P, Zheng Q, et al. Polymeric micelles with dual thermal and reactive oxygen species (ROS)-responsiveness for inflammatory cancer cell delivery. *J Nanobiotechnology*. 2017;15:39. doi:10.1186/s12951-017-0275-4
22. Liu Q, Yang X, Ji J, et al. Novel Nannocystin A analogues as anticancer therapeutics: synthesis, biological evaluations and structure-activity relationship studies. *Eur J Med Chem*. 2019;170:99–111. doi:10.1016/j.ejmech.2019.03.011
23. Yang X, Shi G, Guo J, Wang C, He Y. Exosome-encapsulated antibiotic against intracellular infections of methicillin-resistant Staphylococcus aureus. *Int J Nanomedicine*. 2018;13:8095. doi:10.2147/IJN.S179380
24. Li L, Zhao J-F, Won N, Jin H, Kim S, Chen J-Y. Quantum dot-aluminum phthalocyanine conjugates perform photodynamic reactions to kill cancer cells via fluorescence resonance energy transfer. *Nanoscale Res Lett*. 2012;7:386. doi:10.1186/1556-276X-7-386
25. Ranyuk E, Lebel R, Bérubé-Lauzière Y, et al. (68)Ga/DOTA- and (64) Cu/NOTA-Phthalocyanine Conjugates as Fluorescent/PET Bimodal Imaging Probes. *Bioconjug Chem*. 2013;24:1624–1633. doi:10.1021/bc400257u
26. Liu H-Q, Wang Y-M, Li W-F, et al. Photobleaching characteristics of α-(8-quinolinoxy) zinc phthalocyanine, a new type of amphipathic complex. *Open Chem*. 2017;15:400–411. doi:10.1515/chem-2017-0045
27. Akasov R, Sholina N, Khochenkov D, et al. Photodynamic therapy of melanoma by blue-light photoactivation of flavin mononucleotide. *Sci Rep*. 2019;9:1–11. doi:10.1038/s41598-019-46115-w
28. Naidoo C, Kruger CA, Abrahamse H. Photodynamic Therapy for Metastatic Melanoma Treatment: A Review. *Technol Cancer Res Treat*. 2018;17:1533033818791795. doi:10.1177/1533033818791795
29. Alamzadeh Z, Beik J, Mahabadi VP, et al. Ultrastructural and optical characteristics of cancer cells treated by a nanotechnology based chemo-photothermal therapy method. *J Photochem Photobiol B*. 2019;192:19–25. doi:10.1016/j.jphotobiol.2019.01.005
30. Beik J, Khateri M, Khosravi Z, et al. Gold nanoparticles in combinatorial cancer therapy strategies. *Coord Chem Rev*. 2019;387:299–324. doi:10.1016/j.ccr.2019.02.025
31. Mirrahimi M, Abed Z, Beik J, et al. A thermo-responsive alginate nanogel platform co-loaded with gold nanoparticles and cisplatin for combined cancer chemo-photothermal therapy. *Pharmacol Res*. 2019;143:178–185. doi:10.1016/j.phrs.2019.01.005
32. Wang Z, Gai S, Wang C, et al. Self-assembled zinc phthalocyanine nanoparticles as excellent photothermal/photodynamic synergistic agent for antitumor treatment. *Chem Eng J*. 2019;361:117–128. doi:10.1016/j.cej.2018.12.007
33. Moon HK, Son M, Park JE, Yoon SM, Lee SH, Choi HC. Significant increase in the water dispersibility of zinc phthalocyanine nanowires and applications in cancer phototherapy. *NPG Asia Mater*. 2012;4:e12. doi:10.1038/am.2012.22
34. Li X, Peng X-H, Zheng B-D, et al. New application of phthalocyanine molecules: from photodynamic therapy to photothermal therapy by means of structural regulation rather than formation of aggregates. *Chem Sci*. 2018;9:2098–2104. doi:10.1039/C7SC05115H
35. Doustvandi MA, Mohammadnejad F, Mansoori B, et al. Photodynamic therapy using zinc phthalocyanine with low dose of diode laser combined with doxorubicin is a synergistic combination therapy for human SK-MEL-3 melanoma cells. *Photodiagnosis Photodyn Ther*. 2019;28:88–97. doi:10.1016/j.pdpdt.2019.08.027
36. Gao D, Lo P-C. Polymeric micelles encapsulating pH-responsive doxorubicin prodrug and glutathione-activated zinc(II) phthalocyanine for combined chemotherapy and photodynamic therapy. *J Control Release*. 2018;282:46–61. doi:10.1016/j.jconrel.2018.04.030